International Journal of Scientific Research & Engineering Technology (IJSET)
Vol.6 pp.33-39

Platform Design and Experimental Control of an Unmanned Two-Rotor through PD/PID Controllers

Nada El Gmili [#1], Mostafa Mjahed [*2], Abdeljalil El Kari [#1], Hassan Ayad[#1]

[#] *Department of Applied Physics, Cadi Ayyad University*
Marrakech, Morocco
[1]elgmilinada@gmail.com

[*] *Department of Mathematics and Systems, Royal School of Aeronautics*
Marrakech, Morocco
[2]mjahed.mostafa@gmail.com

***Abstract*— In this paper, we have assembled a small-scale two-rotor Unmanned Aerial Vehicle (UAV). In our design, we propose a simpler platform, which requires only two rotors. Then, a detailed mathematical model is derived using Newton-Euler formalism. Based on this model, roll motion control have been realized efficiently by changing thrust magnitude through PID/PD controllers. Experiments show that the two-rotor is well controlled through the implemented PD/ PID in Ardouino card. Finally, the robustness of the proposed PD controller is demonstrated in presence of wind disturbances.**

***Keywords*— Two-rotor; Twinrotor; UAV; Control; PID; PD**

I. INTRODUCTION

Research and developments related to Unmanned Aerial Vehicles (UAVs) have becoming very active in recent years, motivated by recent technological advances in the fields of miniaturization of actuators and on-board electronics. The design of efficient, low cost UAV systems with autonomous navigation capabilities has become possible. The primary mission of UAVs is to deport the human vision beyond the natural horizon, to accomplish missions at risk or difficult to access for humans [1-3]. Thus, UAVs presents new tools for both civilian and military applications, including agricultural services, natural disaster support, earth science research assistance, hostile zone reconnaissance, border detection, etc. As these applications become more diversified, current research goals have created a serious need to efficiently perform multiple tasks with a single aerial vehicle.

In this work, we are particularly interested to one kind of UAVs having two rotors adjusted in tandem named Two-Rotor. Two-rotor UAVs have been studied recently by many universities and some have designed small prototypes. The first cited in literature was developed at Compiegne University of Technology, named BIROTAN (BI-ROTOR with rotating rotors in TANdem) [4]. Thereafter, other models have emerged [5-9]. In our laboratory, we have assembled a miniaturized two-rotor UAV with a simpler platform. The two-rotor is composed of two rotors radially disposes on the sides opposed. In fact, the moment of each rotor is compensated and the interaction of the two rotors gives a higher load capacity. Unlike conventional helicopters, this configuration does not require swash plate or anti-torque. It is therefore much less complicated mechanically. In addition, the absence of rods makes it possible to reach higher speeds of rotation. In the case of equipment of natural size, tandem rotors are used for the transport of very heavy loads.

The Newton-Euler formalism is used to derive the defining equations of motion of the six Degree Of Freedom system (6-DOF), highly nonlinear, complex and under-actuated with only four control inputs. This complexity makes the control system a delicate task. In addiction to the two-rotor modeling, the aforementioned works [4-9] detail the control system using many strategies. These studies can be summarized as follow: In [4], Kendoul et al presented a model of the complete dynamics and a controller based on the backstepping procedure that is synthesized for autonomous flight. Dickeson et all [5] presented the development and analysis of gain-scheduled, multi-variable H∞ control law for the conversion of a linear parameter varying (LPV) model of a High-Speed Autonomous Rotorcraft Vehicle (HARVee). A nonlinear control scheme, incorporating a function obtained from decoupled dynamics is proposed by Sanchez et al in [6] and applied to the real prototype for hover control. In [7], the authors suggested the design of flight control system for a small unmanned tilt rotor aircraft. Another nonlinear/linearized dynamic and a corresponding design of the altitude tracking controller is developed by Papachristos et al in [8]. Still to perform the control design, Lee et all in [9] proposed an experimental study on time delay control of actuation system of tilt rotor unmanned aerial vehicle. The modeling and control of the two-rotor are also found in [10-15]. Firstly in [10], the author detailled the two-rotor modeling and full control. Then, A. Martini addressed in [11] the system modelling and control .in presence of wind disturbance. After, in [12] Back-stepping control strategy is used for the stabilization of a tilt-rotor UAV. Afterward, some control strategies of a Tilt-rotor UAV are used for Load Transportation in [13]. In [14], the modeling and control of a tiltrotor UAV is developped for path tracking. Where Saeed has detailled in [15] a review on the platform design, dynamic modeling and control of hybrid UAVs. Later in [16], Amiri et al have controlled an unconventional dual-fan unmanned aerial vehicle using Backstepping technique. Therefore, many researchers have developed and controlled aircrafts of type two-rotor, but controlling Two-rotors with PD/PID controllers is new in literature.

The main contribution of our paper lies in the use of PID/PD controller to improve the results concerning the two-

ISSN 2356-5608

rotor control. These controllers reduce significantly the overshoot and the settling time [17]. They offer more robust performance and easy to implement. Also, they do not require a lot of calculations. In the last few years, many projects have controlled quadrotors using PID/PD controllers [18-20]. In [18], Bouabdallah et al have compared PID with LQ control techniques for an indoor micro quadrotor. Then, Salih et al have used in [19] the PID controller in their design for an UAV quadrotor. In [20], authors have used the PDs controllers for the unmanned quadrotor control. After in [21], Zhao has used Neural Network Based PID control for quadrotor aircraft. These controllers have proved their effectiveness for quadrotor control, the reason of why we propose in this work to use these controllers for the two-rotor control. However, PDs/PIDs controllers require a good tuning, so there are several methods to adjust their parameters. Among the classical methods, we find the methods of Ziegler-Nichols [22], Graham-Lathrop [23], Naslin [24], Cohen Coon, the reference model method [25-27], and many other techniques. conventional. Ziegler-Nichols method (Z-N) is used in this work to realize efficient roll motion control.

The remainders of this paper are as follows: In the first section, we detail the platform design and instrumentation. In section II, we present the two-rotor dynamics and roll angle stabilization. In section III, we give the simulation results and demonstrate the robustness of the PD controller in presence of disturbances. In the last section, we give our conclusions.

II. PLATFORM DESIGN

Due to research development, new designs aimed to be more stable and sophistically than the previous ones. The best design is the more stable and the more maneuverable. However, lower stability of design results a complexity in designing the control system. Therefore, the stable flight of an UAV heavily depends on the design [28, 29]. That means that the motion of an UAV depends on the resultant forces and moments applied at the centre of gravity, which is influenced directly by the structure and the design. The Newton-Euler Model shows a good relation of the forces and moments about the centre of gravity of a rigid body.

A. Structure

The structure consists of two brushless DC motors (BLDC), two blades, a gyroscope, a battery, an Arduino UNO card, an Electronic Speed Control (ESC), an aluminum arm, two ball bearings, and a central aluminum chassis. The two ball bearings are coaxial to each other and used to fix a common aluminum arm to the central chassis.

In fig. 1, the motors are arranged with parallel axis of rotation and rest on the two ends of the aluminum arm. They are placed equidistant from the center on opposite sides to cancel the aerodynamic interaction between the propeller blades.

B. Instrumentation

Arduino UNO card: The Arduino card presents the main tool that perform all kinds of actions (start, balance ...). It is able to store data, receive and send information. Arduino module UNO is usually built around an Atmel AVR ATmega328 microcontroller. The module contains a crystal oscillator of 16 MHz (or a ceramic resonator in some models). We use the Arduino card for control, processing and data acquisition.

The gyroscope MPU 6050: The gyroscope MPU 6050 has 6 axes, but we limit the degrees of freedom. This component allows us to have the angle of the two-rotor at every moment.

The brushless motors: The role of the motors is to drive the propellers to create the pushing force. This force is proportional to the speed of the motor. The KV is the rotational speed of an engine for 1 volt. It indicates the number of revolutions / min / volt when the motor turns at no load. The torque is in inverse with the speed, for a fixed power:

- Either have a lot of torque and little speed (low KV).
- Either have a homogeneous distribution of both (average KV).
- Either have more speed and less torque (high KV).

The motors at great KV are heavy energy consumers.

The Electronic Speed Control (ESC): is an electronic circuit dedicated to the control of electric motors. The ESC circuit has a microcontroller (sometimes configurable), a power circuit (regulation, H bridge ...) and in the case of brushless motors, an acquisition device. They allow managing the angular velocity, the direction and the braking.

III. TWIN ROTOR DYNAMICS

A. The rigid body

In order to develop our analysis, let I= (E_1, E_2, E_3) be the Inertial fixed frame and B= (E_x, E_y, E_z) the Body frame. The passage between the body frame B and the inertial frame I is given by the transformation matrix T_R in (1). TR contains the orientation and the position of the mobile frame with respect to the fixed frame. Where R is the rotation matrix (describes the orientation of the mobile object), ξ=[x, y, z] is the position vector. The elements of the rotation matrix R are determined such that R is the product of the rotation matrices around each of the x, y and z axes so it can be parameterized according to the aeronautical Euler angles.

- The first rotation is with angle ψ ($-\pi < \psi < \pi$) around z axis as given in (2).
- The second rotation is with angle θ ($-\pi/2 < \theta < \pi/2$) around y axis as given in (3).
- The third rotation is with angle ϕ ($-\pi/2 < \phi < \pi/2$) around x axis as given in (4).

The formula of the rotational matrix R is given in (5).

$$T_R = \begin{bmatrix} R & \zeta \\ 0 & 1 \end{bmatrix} \quad (1)$$

ISSN 2356-5608

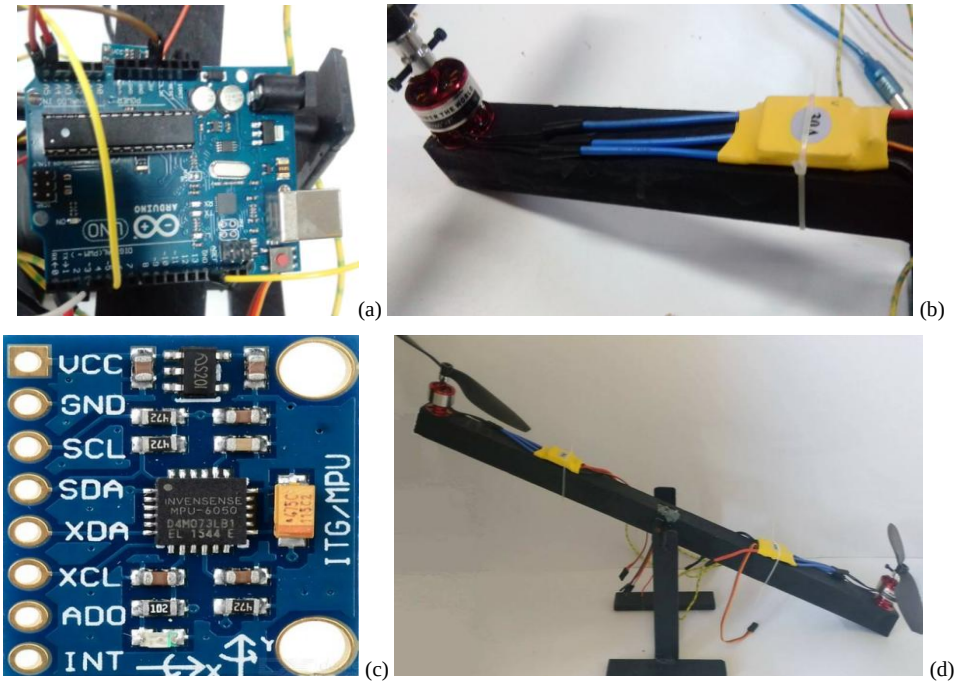

Fig. 1 (a) Controller Ardouino card, (b) ESC and DC motor, (c) Gyroscope, (d) complete assembled model

$$R_{\psi} = \begin{bmatrix} c\psi & -s\psi & 0 \\ s\psi & c\psi & 0 \\ 0 & 0 & 1 \end{bmatrix} \quad (2)$$

$$R_{\theta} = \begin{bmatrix} c\theta & 0 & s\theta \\ 0 & 1 & 0 \\ -s\theta & 0 & c\theta \end{bmatrix} \quad (3)$$

$$R_{\phi} = \begin{bmatrix} 1 & 0 & 0 \\ 0 & c\phi & -s\phi \\ 0 & s\phi & c\phi \end{bmatrix} \quad (4)$$

$$R = R_{\psi} \times R_{\theta} \times R_{\phi}$$

$$= \begin{bmatrix} c\psi\, c\theta & s\phi\, s\theta\, c\psi - s\psi\, c\phi & c\phi\, s\theta\, c\psi + s\psi\, s\phi) \\ s\psi\, c\theta & s\phi\, s\theta\, s\psi + c\psi\, c\phi & c\phi\, s\theta\, s\psi - s\phi\, c\psi \\ -s\theta & s\phi\, c\theta & c\phi\, c\theta \end{bmatrix} \quad (5)$$

Where sx (respectively cx) indicates sin (x) (respectively cos (x)).

B. Forces/Moments acting on the two-rotor

Gravity force:

The gravity force is the force to which the craft is subjected, and whose direction is normal to the surface of the earth. The acceleration of gravity is noted g. Its expression in I is given in (3), where g is the acceleration of gravity. On the surface of the Earth, the gravitational field g is approximately 9, 8 $m.s^{-1}$ at zero altitude.

$$F_G^{\Im} = mG^{\Im} = (0, 0, -mg) \quad (6)$$

Thrust forces:

The thrust forces are perpendicular to the plane of the propellers. These forces are proportional to the square of the rotational velocity of the motors. The expression of the total thrust in the reference B linked to the two-rotor is given in (8), Where C_l is the thrust coefficient, ω_1 and ω_2 are the rotational speed of the rotors 1 and 2 respectively and $P=P_1+P_2$.

$$\begin{cases} P_1 = C_l\ \omega_1^2 \\ P_2 = C_l\ \omega_2^2 \end{cases} \quad (7)$$

$$F_T^B = P_1^B + P_2^B = \begin{pmatrix} 0 \\ 0 \\ P \end{pmatrix} \quad (8)$$

Axial drag force:

In the horizontal movement, the rotor is deflected by the fuselage, creating a drag force along the x, y and z axes added to the drag force induced by the speed. The effect of this force on the body during the movement is modeled in the reference linked to the body B as follows:

ISSN 2356-5608

$$F_{Dax}^{B} = \begin{bmatrix} -\frac{1}{2}C_{Dx}A_x\rho\dot{x}|\dot{x}| & 0 & 0 \\ 0 & -\frac{1}{2}C_{Dy}A_y\rho\dot{y}|\dot{y}| & 0 \\ 0 & 0 & -\frac{1}{2}C_{Dz}A_z\rho\dot{z}|\dot{z}| \end{bmatrix} = \begin{bmatrix} -K_{fax} & 0 & 0 \\ 0 & -K_{fay} & 0 \\ 0 & 0 & -K_{faz} \end{bmatrix} \dot{\xi}^2(t) \quad (9)$$

Where

- C_{Dx}, C_{Dy}, C_{Dz} represent the axial drag coefficients in the x, y and z directions, respectively;
- A_x, A_y, A_z are the cross sections of the Bicopter Tandem ;
- -1/2 C_{Dx} A_x ρ, -1/2 C_{Dy} A_y ρ, -1/2 C_{Dz} A_z ρ are considered as aerodynamic coefficients of friction representing K_{fax}, K_{fay}, K_{faz}, respectively.

Actuators torque:

The position vectors of the points of application of the thrusts P_1 and P_2, expressed in B, are $(0, -l\ , 0)$ and $(0, l\ , 0)$, respectively. Therefore, the torque produced by the thrusts relative to the center of gravity G expressed in B is given in (6), where $u_\phi = l/2\ (P_2 - P_1)$.

$$M_A^B = \begin{pmatrix} 0 \\ -l/2 \\ 0 \end{pmatrix} \times P_1^B + \begin{pmatrix} 0 \\ l/2 \\ 0 \end{pmatrix} \times P_2^B = \begin{pmatrix} u_\phi \\ 0 \\ 0 \end{pmatrix} \quad (10)$$

C. The two-rotor dynamics

The two-rotor dynamics can be modelled using Newton Euler formulation:

$$m\ddot{\xi} = F^{\Im} \quad (11)$$

$$I\dot{\Omega} + \Omega \times I\Omega = M^B \quad (12)$$

Where

- $\dot{\xi} = (\dot{x},\ \dot{y},\ \dot{z})^T \in R^3$ is the velocity vector of the two-rotor;
- m is the total mass of the two-rotor;
- $F^{\Im} \in R^3$ is the sum of forces expressed in I;
- $I \in R^{3\times3}$: Symmetrical inertia matrix;
- Ω: The angular velocity expressed in I;
- x: The vector product;
- $M^B \in R^3$: The total external moment expressed in B.

The total force $F^{\Im}$ acting on the center of gravity of the system is the sum of the force of gravity $F_g^{\mathbf{E}}$, the thrust forces $F_T^{\Im}$ created by the rotors, and the aerodynamic forces F_{Dax}^{E}. According to the balance of forces, the resultant of the total forces is written:

$$\begin{aligned} F^{\Im} &= F_g^{\Im} + F_T^{\Im} + F_{Dax}^{\Im} \\ &= (0,0,-mg) + R \times F_T^B + R \times F_{Dax}^B \end{aligned} \quad (13)$$

To better understand this model for control analysis, we chose to work with a reduced dynamic model where the inertia matrix and the mass of the vehicle are normalized, and F_{Dax}^B is considered a disturbance. The differential equations that define the translational and rotational motion are given in (14).

$$\begin{cases} \ddot{x} = P\ \sin\psi\ \sin\phi + P\ \cos\psi\ \sin\theta\ \cos\phi \\ \ddot{y} = P\ \sin\psi\ \sin\theta\ \cos\phi - P\ \cos\psi\ \sin\phi \\ \ddot{z} = P\ \cos\theta\ \cos\phi - g \\ \ddot{\phi} = u_\phi \end{cases} \quad (14)$$

IV. Roll Motion Control

A. Roll motion

The roll motion is controlled by the difference in the angular velocity of the two rotors. The motor that rotates with a higher velocity produces a higher thrust, thus creating a rolling effect in an opposite direction. The altitude is regulated by increasing or decreasing the thrust of the rotors.

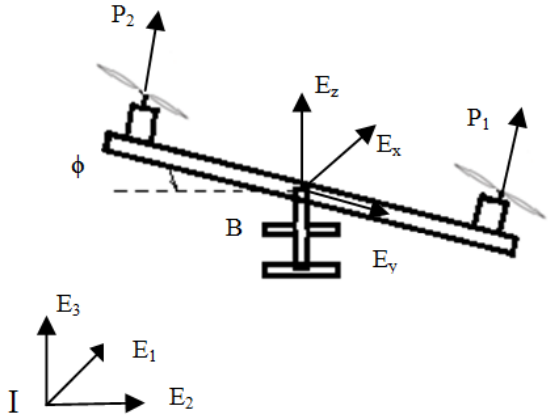

Fig. 2 Roll motion

B. Roll control

The two-rotor can be controlled by modifying the thrust of each motor to keep closer to the desired position. For this, we use PID controller (Proportional, Integral, Derivative). Some of the advantages of the PID/PD controller are its simplicity and ease of implementation. In many research papers, PID/PD control technique has been proposed in control system [30-32]. However, its parameters need a good tuning.

ISSN 2356-5608

The transfer function of the PID controller C(p) and its parameters (K_p, K_i and K_d) are as specified in (15), where C_p, C_i and C_d are the proportional, integral and derivative actions, respectively.

$$C(p) = \frac{u(p)}{\varepsilon(p)} = K_p + \frac{K_i}{p} + K_d\, p \qquad (15)$$

The Ziegler-Nichols (Z-N) closed loop method is used to tune the controllers' parameters. However, this method requires the linear transfer function of the system to control. By applying the Laplace transform to the roll equation defined in (16), we obtain the following transfer function of roll angle.

$$F_\phi(p) = \frac{(P_2 - P_1)}{\phi} = \frac{l/2}{p^2} \qquad (16)$$

The critical gain K_c and the critical period T_c correspond to an oscillatory behavior of the closed loop transfer function. To find the value of K_c, a proportional gain corrector K_p is brought into a closed loop in series with the system to correct. Then, there are two ways: either increase the gain K_p until the system goes into oscillation or calculate the transfer function of the closed-loop PID controller and obtain the value of the critical gain K_c from Routh criterion. The value T_c corresponds to the oscillations period of the closed loop system response.

Table I gives the Z-N proposed parameters of PID/PD gains.

TABLE I
PD/PID PARAMETERS BASED ON CLOSED LOOP Z-N METHOD

Controller	**K_p**	**K_i**	**K_d**
PD	0.71 K_c	-	0.15 T_c
PID	0.6 K_c	0.5 T_c	0.125 T_c

V. SIMULATION RESULTS & TEST

The parameters for the complete assembled two-rotor are given in Table II. For a reference step signal, we obtain the response of the roll angle in closed loop in fig. 3.

From this figure, it is clearly shown that the system present a high overshoot and needs to be controlled. To provide an appropriate control for the two-rotor, we use Proportional, Integral and Derivative actions. The derivative action is employed to improve the transient responses of these transfer functions in closed-loop. However, it does not have any effect on the steady-state performance of the closed loop responses. Moreover, single derivative control is not used because it amplifies high-frequency noise which is never desired. As consequence, we use PD/PID controller. One of the advantages of these controllers is that they can be easily implemented experimentally. The PID/PD parameters that kept the system the most possible stable are obtained by applying Z-N method to the transfer function defined by (10). These parameters are summarized in table III.

TABLE II
THE PARAMETERS FOR THE TWO-ROTOR

Parameter	**value**
G (m. s^{-1})	0.98
l (m)	0.80

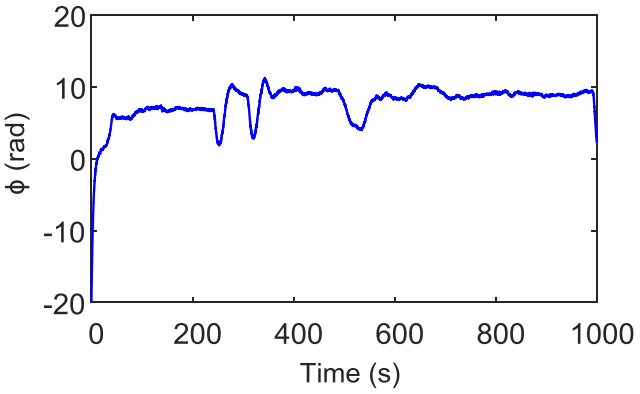

Fig. 3 Step response of the roll angle in closed loop

TABLE III
PD/PID PARAMETERS OBTAINED BY USING ZN

Controller	**K_p**	**K_i**	**K_d**
PD	2.5	-	0.81
PID	2.1	2.7	0.675

The content of the arduino program is divided into three parts:

Declaration: In this part we put the declaration of the libraries to use, including the servo motor library "#include <Servo.h>" and the communication library "#include <Wire.h>".

Void setup: In this part, the different input/output pins are defined. It includes, also, a loop for the calibration of the motors, which is done referring to the basic example of the gyroscope given in the Arduino library.

Void loop: This part works as an infinite loop, in which we put the desired angle calculation, PID control and motor control instructions.

The gyroscope gives the roll angle value. Then, we calculate the actual error (AE) between the desired and the received value. The proportional value C_p is just the gain K_p multiplied by the error as shown in (17). The integral and derivative values C_i and C_d are obtained from (18) and (19), where PE and PT are the previous error and the previous time. PT is stored before the actual time (AT) read.

$$C\_p = K_p\, E \qquad (17)$$

$$C\_i = K_i\, PE + K_i\, E \qquad (18)$$

$$C\_d = K_d\, ((E\text{-}PE)/(AT\text{-}PT) \qquad (19)$$

ISSN 2356-5608

The PID value is the sum of the three proportional, integral and derivative values according to (20). This action is limited to not exceed the nominal speed of the motors. We calculate the PWM width of each pulse. Then, we calculate the sum of the desired throttle and the PID value according to (21) and (22). Finally, using the servo function, we create the PWM pulses with the calculated width for each pulse and we store the previous error (PE) and the loop recommence. The results obtained based on the PID and those based on PD parameters obtained by Z-N in table III are presented in figures 4 and 5.

$$PID=C\_p+C\_i+C\_d \quad (20)$$

$$pwmLeft=P_1+PID \quad (21)$$

$$pwmRight=P_2-PID \quad (22)$$

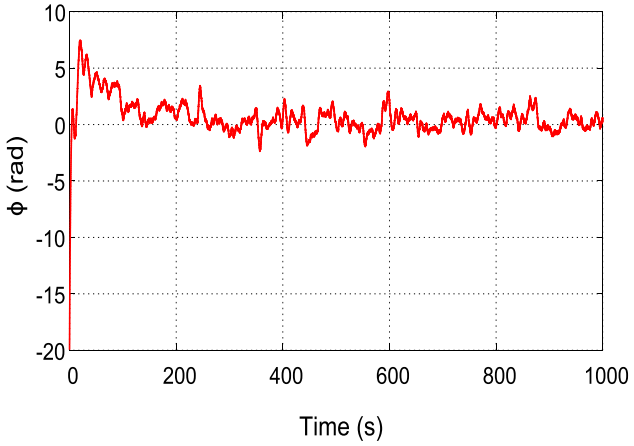

Fig. 4 Step response of the roll angle with PID controller in closed loop

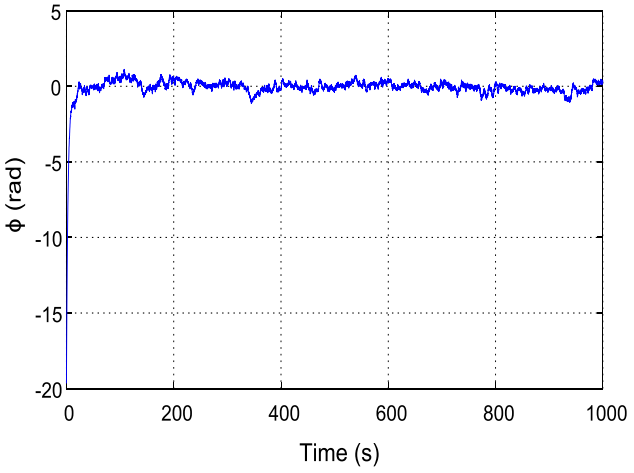

Fig. 5 Step response of the roll angle with PD controller in closed loop

It can be noticeably observed from fig. 5 that the PD controller stabilizes the roll angle response with a short overshoot compared to the PID controller. These results are obtained since the roll transfer function in (29) has already an integration. As consequence, we use the PD controllers to provide the appropriate control of the roll variations of the two-rotor.

Moreover, to evaluate the efficiency of the PD controller, the real system with PD controller is tested experimentally. The results obtained when the two-rotor is controlled for a desired trajectory (input signal) are depicted in Fig. 6, where the simultaneous changes in the reference input signal are efficiently followed with a short overshoot.

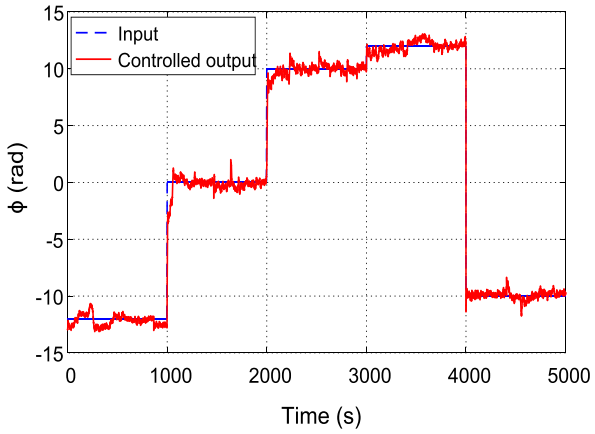

Fig. 6 Corrected response in closed loop for variable roll angle input

To test the robustness of this controller, external disturbances have been injected [33]. The most likely disturbance acting on the two-rotor is the wind disturbance. A test has been done when the desired reference roll angle has variable values. According to fig. 7, the PD controller rejected the undesired effects of the disturbance and results an output signal close to the reference one.

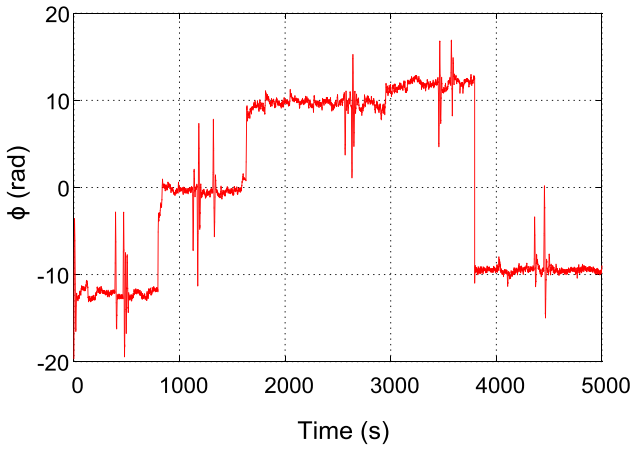

Fig. 7 Corrected response in closed loop for variable roll angle input in presence of wind disturbances

VI. Conclusions

In this paper, a platform design and an experimental control of the two-rotor UAV have been proposed. First, a minimized two-rotor UAV has been designed through a simpler platform and a description of all the parts comprising the development of the two-rotor has been presented. Second, forces and moments acting on the aircraft dynamics were clearly explained and the mathematical model has been clearly developed using Newton-Euler formalism. Third, the

ISSN 2356-5608

experimental control of roll motion is realized efficiently by using PID/PD controller. The controller parameters have been tuned using the conventional method of Ziegler-Nichols (Z-N).

Experimental simulations carried out on the roll control show us that the PD is more efficient than the PID controller for the two-rotor control. Indeed, the robustness of this controller is proved in presence of disturbances.

REFERENCES

[1] D. Poinsot, "Commande d'un drone en vue de la conversion vol rapide-vol stationnaire," doctoral thesis, Ecole nationale superieure de l'aeronautique et de l'espace, amien, 2008.

[2] J. A. Escareno-Castro, "Conception, modélisation et commande d'un drone convertible, " doctoral thesis, Compiègne, 2008.

[3] A. Koel, "Modélisation, observation et commande d'un drone miniature à birotor coaxial," doctoral thesis, Université Henri Poincaré-Nancy I, 2012.

[4] F. F. Kendoul, "Modeling and control of a small autonomous aircraft having two tilting rotors," *IEEE Transactions on Robotics*, vol. 22(6), pp. 1297-1302, 2005.

[5] J. J. Dickeson, "Robust LPV H∞ gain-scheduled hover-to-cruise conversion for a tilt-wing rotorcraft in the presence of CG variations," *Decision and Control, 2007 46th IEEE Conference*, 2007, p. 2773-2778.

[6] A. E. Sanchez, "Autonomous hovering of a noncyclic tiltrotor UAV: Modeling, control and implementation", *IFAC Proceedings Volumes*, vol. 41(2), pp. 803-808, 2008.

[7] S. E.Yanguo, "Design of flight control system for a small unmanned tilt rotor aircraft," *Chinese Journal of Aeronautics*, vol. 22(3), pp. 250-256, 2009.

[8] C. A. Papachristos, "Design and experimental attitude control of an unmanned tilt-rotor aerial vehicle," *Advanced Robotics (ICAR), 2011 15th International Conference on. IEEE*, 2011, p. 465-470.

[9] J. Y. Lee, "An experimental study on time delay control of actuation system of tilt rotor unmanned aerial vehicle," *Mechatronics*, vol. 22(2), pp. 184-194, 2012.

[10] I. Fantoni-Coichot, *Vers l'autonomie des véhicules aériens.* Mémoire pour l'Habilitation à Diriger des Recherches, 2007.

[11] A. Martini, "Modélisation et commande de vol d'un hélicoptère drone soumis à une rafale de vent.Metz," doctoral thesis, 2008.

[12] A. B. Chowdhury, "Back-stepping control strategy for stabilization of a tilt-rotor uav". *Control and Decision Conference (CCDC), 2012 24th Chinese IEEE*, pp. 3475-3480, 2012.

[13] M. M. De almeida neto, "Control Strategies of a Tilt-rotor UAV for Load Transportation", 2014.

[14] R. R. Donadel, "Modeling and control of a tiltrotor uav for path tracking". *47*(3), pp. 3839-3844, 2014.

[15] A. S. Saeed, "A review on the platform design, dynamic modeling and control of hybrid UAVs," *Unmanned Aircraft Systems (ICUAS), 2015 International Conference on. IEEE*, pp. 806-815, 2015.

[16] N. Amiri, A. Ramirez-Serrano, R. J. Davies, "Integral backstepping control of an unconventional dual-fan unmanned aerial vehicle". *Journal of Intelligent & Robotic Systems*, *69*(1-4), pp. 147-159, 2013.

[17] K. J. Astrom, *PID controllers: theory, design and tuning*, Instrument society of America, 1995.

[18] S. Bouabdallah, A. Noth, & R. Siegwart, "PID vs LQ control techniques applied to an indoor micro quadrotor". *International Conference in Intelligent Robots and Systems IEEE, IROS 2004*, vol. 3, pp. 2451-2456,2004.

[19] A. L. Salih, M. Moghavvemi, H. Mohamed, K. S. Gaeid, "Flight PID controller design for a UAV quadrotor", *Scientific Research and Essays*, vol. 5(23), pp. 3660–3667, 2010.

[20] Y. Naidoo, R. Stopforth, G. Bright, "Quadrotor Unmanned Aerial Vehicle Helicopter Modelling & Control," *International Journal of Advanced Robotic Systems*, vol. 8(4), pp. 139-149, 2011.

[21] D. S. Zhao, "Neural Network Based PID Control for Quadrotor Aircraft," *International Conference on Intelligent Science and Big Data Engineering. Springer International Publishing*. pp 287-297, 2015.

[22] K. J. Astrom, T. Hagglund, "Revisiting the Ziegler-Nichols step response method for PID control". Journal of process control, vol14, no 6, 635-650, 2004.

[23] D. Graham, R. C. Lathrop, "The synthesis of optimum transient response: Criteria and standard forms", Transactions AIEE, II, vol 72 no 5, 273-288, 1953.

[24] P. Naslin, "Essentials of optimal control". Iliffe& Sons Ltd, London,1968.

[25] M. Mjahed, Commande des systèmes, Lectures Notes, Ecole Royale de l'Air, Marrakech, 2016.

[26] N. El gmili, M. Mjahed, A. EL Kari, H. Ayad,"An Improved Particle Swarm Optimization (IPSO) Approach for Identification and Control of Stable and Unstable Systems". International Review of Automatic Control (IREACO), vol 10, no 3, 229-239, 2017.

[27] I. Siti, M. Mjahed, H. Ayad, A. EL Kari, "New Designing Approaches for Quadcopter PID controllers using Reference Model and Genetic Algorithm techniques". International Review of Automatic Control (IREACO), vol 10, no 3, 240-248, 2017.

[28] A. A. Shlok, "Design, construction and structure analysis of twinrotor UAV," vol *4*(3), pp 33-42, 2014.

[29] F. S. Goncalves, "Small scale uav with birotor configuration". In Unmanned *Aircraft Systems (ICUAS), 2013 International Conference on IEEE*, pp. 761-768, 2013.

[30] G. Kasilingam, J. Pasupuleti, "Coordination of PSS and PID controller for power system stability enhancement–overview," *Indian Journal of Science and Technology*, vol. 8(12), pp. 1-10, 2015.

[31] T. Deif, and al, "Modeling and Attitude Stabilization of Indoor Quad Rotor," *International Review of Aerospace Engineering (IREASE)*, vol.7 (2), pp. 43-47, 2014.

[32] S. Aghajani, I. Joneidi, M. Kalantar, V. M. Apour, "Modeling and simulation of a PV/FC/UC Hybrid Energy System for Stand Alone Applications," *International Journal on Energy Conversion (IRECON)*, vol. 2 (1), pp.26-34, 2014.

[33] R. Xia Guo, J. Kang Dong et Y. Zhu, "Disturbance Rejection and Asymptotically Stabilizing Control for a Quadrotor UAV," *Journal of Control Engineering and Applied Informatics*, vol. 17 (4), pp. 33-41, 2015.

ISSN 2356-5608